

Search for HBr and bromine photochemistry on Venus



Vladimir A. Krasnopolsky^{a,1,*}, Denis A. Belyaev^b

^a *Moscow Institute of Physics and Technology (PhysTech), Dolgoprudniy, Russia*

^b *Space Research Institute, Russian Academy of Sciences, Moscow, Russia*

ARTICLE INFO

Article history:

Received 28 November 2016

Revised 19 February 2017

Accepted 18 April 2017

Available online 19 April 2017

ABSTRACT

HBr (1–0) R2 2605.8/6.2 cm^{-1} , the strongest line of the strongest band of HBr, was observed when searching for this species on Venus. The observation was conducted using the NASA IRTF and a high-resolution long-slit spectrograph CSHELL with resolving power of 4×10^4 . 101 spectra of Venus were analyzed, and the retrieved HBr abundances varied from -8 to $+5$ ppb. Their mean value is -1.2 ppb, standard deviation is 2.5 ppb, and uncertainty of the mean is 0.25 ppb. The negative value presumes a systematic error, and the estimated upper limit of the HBr mixing ratio at the cloud tops of Venus is ~ 1 ppb. From the simultaneously retrieved CO_2 abundances, this corresponds to an altitude of 78 km for the uniform distribution of HBr. A simplified version of the bromine photochemistry is included into the photochemical model (Krasnopolsky 2012, Icarus 218, 230–246). Photolysis of HBr and its reactions with O and H deplete the HBr mixing ratio at 70–80 km relative to that below 60 km by a factor of ≈ 300 . Reanalysis of the observational data with the calculated profile of HBr gives an upper limit of 20–70 ppb for HBr below 60 km and the aerosol optical depth of 0.7 at 70 km and 3.84 μm .

The bromine chemistry may be effective on Venus even under the observed upper limit. However, if a Cl/Br ratio in the Venus atmosphere is similar to that in the Solar System, then HBr is ≈ 1 ppb in the lower atmosphere and the bromine chemistry is insignificant. Thermodynamic calculations based on the chemical kinetic model (Krasnopolsky 2013, Icarus 225, 570–580) predict HBr as a major bromine species in the lower atmosphere.

© 2017 Published by Elsevier Inc.

1. Introduction

The surface of Venus and the nearby atmosphere are very hot, and some rocks may have saturated vapor pressures that contribute to the atmospheric composition (for example, iron chloride Krasnopolsky, 2017a). The high temperature stimulates reactions between rocks and atmospheric species that may release exotic volatiles like HCl and HF, which looked very unusual when they were detected by Connes et al. (1967). One may expect that the next hydrogen halide, hydrogen bromide HBr, may exist in measurable quantities in the Venus atmosphere as well. However, we have not found any attempts to detect this species in the literature. The only result relevant to bromine on Venus is an upper limit of 0.2 ppb to Br_2 near 15 km from the spectrophotometric observa-

tions at the Venera 11 and 12 descent probes (Moroz et al., 1981). Our search for HBr on Venus is the subject of this study.

2. Observations

Bromine has two isotopes, ^{79}Br and ^{81}Br , with almost equal relative abundances, 0.507 and 0.493, respectively. The difference between the reduced masses of the HBr isotopologues is small, and each line of HBr has two isotopic components. The fundamental band (1–0) is stronger than the first overtone (2–0) by a factor of 92 and is a better candidate to search for HBr. Its lines R2 at 2605.80 and 2606.20 cm^{-1} have strengths of $\approx 8 \times 10^{-20}$ cm at 200–220 K that are the strongest in the band. The former is in a clean spectral interval that is not contaminated by telluric, solar, and Venusian lines. These HBr lines are subject of our search. Though the lines are strong, they are weaker than the similar HCl and HF lines by factors of 8 and 36, respectively (HITRAN 2012, Rothman et al., 2013). This makes our task more difficult.

We observed Venus on July 16, 2015, using the NASA Infrared Telescope Facility (IRTF) on Mauna Kea, Hawaii, with elevation of 4.2 km and mean overhead water of 2 precipitable mm. The telescope with diameter of 3 m was coupled with a long-slit high-

* Corresponding author.

E-mail address: vlad.krasn@verizon.net (V.A. Krasnopolsky).

¹ Visiting Astronomer at the Infrared Telescope Facility, which is operated by the University of Hawaii under Cooperative Agreement No. NCC 5-538 with the National Aeronautic and Space Administration, Science Mission Directorate, Planetary Astronomy Program.

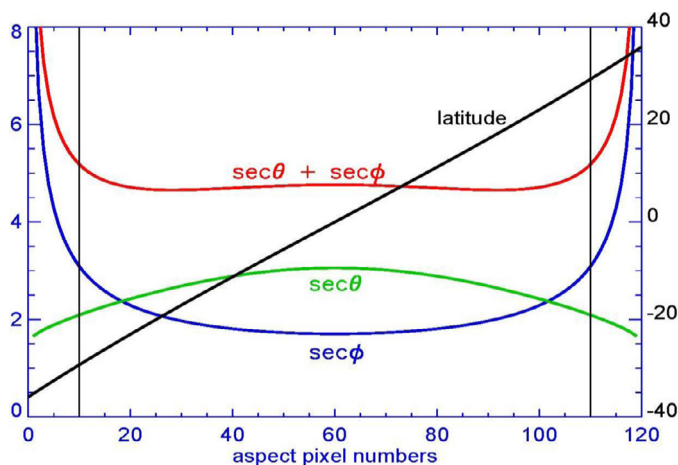


Fig. 1. Latitudes (right scale), secants of the solar zenith angle θ and observing angle ϕ , and their sums, that is, airmasses for 121 observed spectra of Venus. 101 spectra restricted by vertical lines are chosen for analysis.

resolution spectrograph CSHELL (Greene et al., 1993). It operates in the range 1.1 to 5.6 μm with a resolving power $\nu/\delta\nu \approx 4 \times 10^4$. The instrument detector is a InSb array of 256×150 pixels that is cooled to 30 K. Each pixel is equal to $9 \times 10^{-6} \nu_0$ in the dispersion direction and 0.2 arcs in the aspect direction. Here ν_0 is a chosen mean wavenumber, and spectral coverage is $0.0023 \nu_0$ with the slit length of 30 arcs. The slit width is 0.5 arcs, and each row on the detector is a spectrum of the proper point on the slit.

The angular diameter of Venus was 40.9 arcs, and its heliocentric and geocentric velocities were 0.15 and -11.4 km s^{-1} . Phase (Sun-Venus-observer) angle was 125° , and the bright crescent of Venus was 0.43 of its radius. The slit was placed near the middle of the bright crescent tangential to the limb. Spectra of Venus, nearby sky foreground (1 arcmin off Venus center), dark current, and flat field from a continuum light source were acquired.

3. Data analysis and results

The spectra of the sky foreground were subtracted from the Venus spectra that then were divided by the difference between the flat field and dark current spectra. This operation removes their effects on the Venus spectra. Then bad pixels were replaced by mean values of their neighbors.

The slit is a chord that is 24 arcs long on Venus. Therefore we observed 121 spectra along this chord. Calculated latitudes, secants of the solar zenith angle θ and the observing angle ϕ , and their sum are shown in Fig. 1. This sum is airmass that is almost constant at 4.8 for the central 101 spectra and steeply increases to the limb beyond these spectra. We will analyze the 101 middle spectra (Fig. 1).

The central wavenumber is $\nu_0 = 2606 \text{ cm}^{-1}$, and the spectral coverage is $2603\text{--}2609 \text{ cm}^{-1}$. We choose a spectral interval of 2604.6 to 2607.1 cm^{-1} for analysis. This interval includes the strongest HBr (1–0) R2 lines at 2605.80 and 2606.20 cm^{-1} that are Doppler-shifted by 0.099 cm^{-1} .

Our technique for fitting the observed spectra by synthetic spectra involves conversion of the observed spectra to a scale with a wavenumber step of 0.001 cm^{-1} . This is done by parabolic fitting of three adjacent pixels to transform a pixel value into eight sampling points that keep the sum of those points at the pixel value. The spectra include four strong Doppler-shifted CO_2 lines from the Venus atmosphere. These lines were used for wavenumber calibration of the spectra. Then the spectra were linearly interpolated to

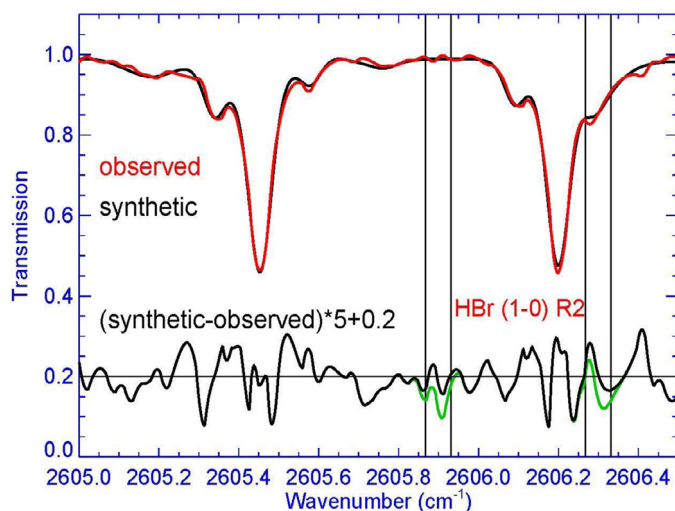


Fig. 2. Observed and synthetic spectra of Venus at the equator. Vertical lines show resolution elements at the expected positions of the Doppler-shifted HBr lines. The black line near the bottom shows a difference between the synthetic and observed spectra scaled by a factor of 5 and shifted to 0.2 for convenience. The green line is the same but for an HBr abundance of 10 ppb. (For interpretation of the references to colour in this figure legend, the reader is referred to the web version of this article.)

scales with the step of 0.001 cm^{-1} , and we further reduced the spectral interval to $2604.9\text{--}2606.6 \text{ cm}^{-1}$.

Our fitting procedure involves further adjustments to the spectra. Venus reflectivity, the solar continuum, and the instrument sensitivity may slightly vary within the spectral interval, and we applied a parabolic correction (three fitted parameters) to compensate for these effects. Minor errors in the wavenumber scale result in significant differences between the observed and synthetic spectra for strong absorption lines, and we used wavenumber corrections at the edges and in the middle of the observed spectra, that is, six fitting parameters per spectrum. The corrected spectrum observed at the equator is shown by the red line in Fig. 2.

We use a version of a high-resolution solar spectrum from Kurucz (2011) that is based on the ATMOS spectrum (Farmer and Norton 1989). The observed spectra include two strong CO_2 lines and a few weaker but prominent CO_2 lines. These lines are venusian and calculated using the Voigt line shape. Two lines are essential in the Earth's atmosphere, though the CO_2 abundance above Mauna Kea is smaller than the observed slant Venus abundances by a factor 200. Two parameters, abundance and temperature, are applied to CO_2 on Venus, and pressure is calculated using the adopted CO_2 abundance. The telluric CO_2 , H_2O , CH_4 , and N_2O lines are calculated with the known terrestrial data and abundances of H_2O and CH_4 as free parameters. The calculated spectra are convolved by a Gaussian with a variable spectral resolution. The convolution further reduces the spectral interval to $2605.0\text{--}2606.5 \text{ cm}^{-1}$ (Fig. 2). The number of parameters to calculate a synthetic spectrum (Fig. 2) is six, and the total number of fitting parameters is 12. The number of degrees of freedom is equal to the number of pixels in the spectral interval, that is, 64.

Standard deviation is 0.5% for the difference between the synthetic and observed at $2605.6\text{--}2606.0 \text{ cm}^{-1}$ around the first HBr line. The difference in the line is smaller than the standard deviation and corresponds to a negative HBr abundance of -0.5 ppb. A spectrum calculated for the abundance of 10 ppb is shown in Fig. 2 as well. The difference at the line position is 1.3% for this spectrum, that is, 10 ppb corresponds to 2.6 sigma detection for a single spectrum. The data from 101 spectra reduces the detection limit to 1 ppb.

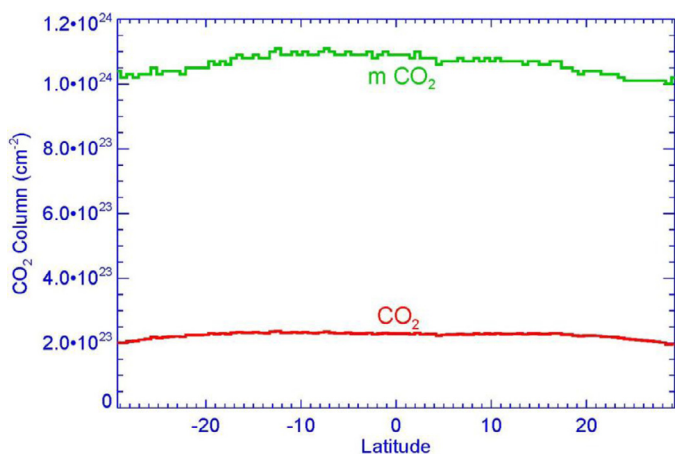


Fig. 3. Retrieved column abundances of CO₂ (uncorrected and corrected for air-mass) in the sounded atmospheric layer.

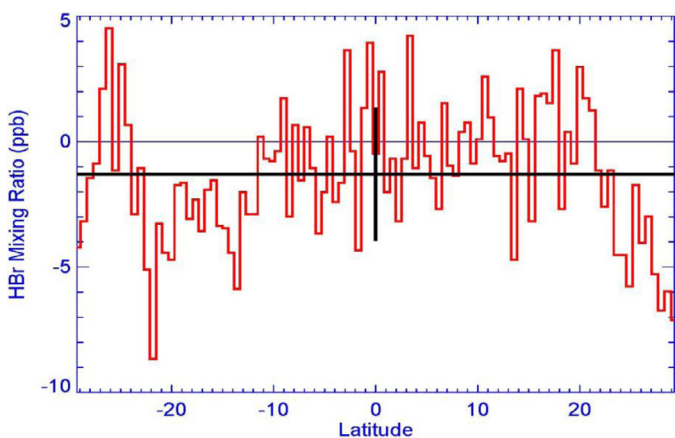


Fig. 4. Retrieved HBr mixing ratios in the observed 101 spectra of Venus. The mean value and standard deviation of the data distribution are shown by black solid lines.

Retrieved abundances of CO₂ uncorrected and corrected for air-mass are shown in Fig. 3. The corrected values are rather constant and result in pressure of 14 mbar at the bottom of the sounded atmospheric layer. Our data for Venus refer to a half pressure level of 7 mbar, which is at 78 km according to VIRA (Seiff et al. 1985). The observed abundance of telluric water above Mauna Kea is 1.2 pr. mm, smaller than the mean abundance of 2 pr. mm.

Derived HBr and CO₂ column abundances are converted into HBr mixing ratios in Fig. 4. The scatter of the results is large with a mean value of -1.2 ppb and standard deviation of 2.5 ppb. If the data conform the Gauss statistics, that is, their distribution is random, then uncertainty of the mean of 101 values is smaller by a factor of 10 and equal to 0.25 ppb. The negative mean abundance exceeding the uncertainty indicates effect of possible systematic errors. Our evaluation of an upper limit to the HBr mixing ratio is ~1 ppb at 78 km on Venus.

4. Possible bromine photochemistry on Venus

To understand and establish the bromine photochemistry on Venus, it is helpful to compare bond energies of the simplest Br species with those of some other important species on Venus (Table 1).

The HBr dissociation energy is smaller than that of HCl, its absorption cross sections are larger and extend up to 230 nm. The

Table 1
Bond energies of bromine and some other species.

| Species | HBr | Br ₂ | BrO | HCl | H ₂ | H-OH | OH | H-O ₂ | NO-O |
|---------|------|-----------------|------|------|----------------|------|------|------------------|------|
| E (eV) | 3.80 | 2.00 | 2.47 | 4.48 | 4.48 | 5.14 | 4.39 | 2.0 | 3.12 |

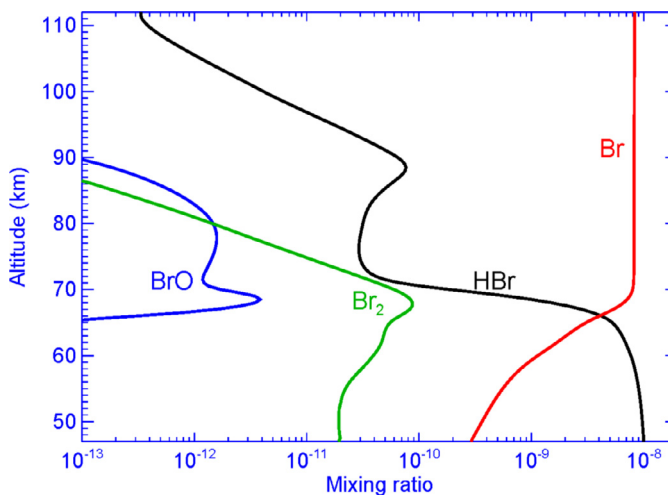
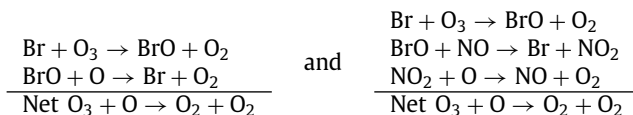


Fig. 5. Vertical profiles of bromine species in the photochemical model.

HBr bond energy is smaller than those of H₂ and OH as well, and HBr is lost in reactions with O and H (Table 2) that are ineffective for HCl. Similar to HCl, HBr is delivered by eddy diffusion from the lower atmosphere and formed by the reaction of Br + HO₂ and the termolecular association. Bromine cycles that produce O₂ are



They are similar to those of Cl. However, the ClCO cycle that provides recombination of CO + O₂ does not have a bromine analog. Termolecular association and fast photolysis of Br₂ by the visible light determine its balance in our simplified scheme. The existence of bromine is questionable in the Venus atmosphere, and here we do not include reactions between bromine and nitrogen and chlorine species.

Ten bromine reactions from Table 2 are included into the photochemical model by Krasnopolsky (2012) that was recently updated (Krasnopolsky 2017b) using new data on the S₂O₂ photolysis. The model is calculated assuming the HBr mixing ratio of 10 ppb at the model lower boundary of 47 km. The calculated vertical profiles of the bromine species are shown in Fig. 5.

Photolysis and the reactions with O and H steeply reduce the HBr mixing ratio above 67 km. The fast photolysis of Br₂ and the reactions of BrO with O and NO convert these species to Br, which dominates above 67 km. The most significant effect of the bromine chemistry is in the production of H₂ (reaction 3), which exceeds that without Br by a factor of 5, and in the production of O₂, which is a third of that without Br.

5. Discussion

We have already mentioned above that the strongest HBr lines are weaker than those of HCl and HF by factors of 8 and 36, respectively. Taking this fact into account, the derived upper limit of 1 ppb to HBr at 78 km is very sensitive. Scaling it to HF, it corresponds to HF detectivity of 0.03 ppb.

Table 2
Bromine reactions, rate coefficients, column rates (CR), mean altitudes (km), and CR for chlorine analogs.

| # | Reaction | Rate Coefficient | Reference | CR | <i>h</i> | CR (Cl) |
|----|---|--|-------------------------|-----------|----------|-----------|
| 1 | HBr + <i>hν</i> → H + Br | – | Sander et al. (2011) | 3.27 + 10 | 68 | 9.46 + 10 |
| 2 | HBr + O → Br + OH | $5.8 \times 10^{-12} e^{-1500/T}$ | DeMore et al. (1997) | 1.15 + 10 | 68 | 1.60 + 9 |
| 3 | HBr + H → Br + H ₂ | $1.7 \times 10^{-11} (T/300)^{0.5} e^{-300/T}$ | Mitchell et al., (1995) | 1.30 + 10 | 71 | 2.31 + 9 |
| 4 | H + Br + M → HBr + M | $5 \times 10^{-31} (300/T)^{1.87}$ | Baulch et al., (1981) | 1.47 + 10 | 73 | – |
| 5 | Br + HO ₂ → HBr + O ₂ | $7.7 \times 10^{-12} e^{-450/T}$ | Atkinson et al. (2007) | 4.12 + 10 | 67 | 6.71 + 10 |
| 6 | Br + O ₃ → BrO + O ₂ | $1.7 \times 10^{-11} e^{-800/T}$ | Atkinson et al. (2007) | 2.16 + 12 | 69 | 6.89 + 12 |
| 7 | BrO + O → Br + O ₂ | $1.9 \times 10^{-11} e^{230/T}$ | Atkinson et al. (2007) | 4.35 + 11 | 74 | 3.50 + 12 |
| 8 | BrO + NO → Br + NO ₂ | $8.7 \times 10^{-12} e^{260/T}$ | Atkinson et al. (2007) | 1.73 + 12 | 68 | 4.22 + 12 |
| 9 | Br + Br + M → Br ₂ + M | $10^{-32} (300/T)^{2.77}$ | Donohoue et al., (2006) | 1.04 + 14 | 57 | 1.64 + 13 |
| 10 | Br ₂ + <i>hν</i> → Br + Br | 0.03 s ⁻¹ | Sander et al. (2011) | 1.04 + 14 | 57 | 3.18 + 13 |

Rate coefficients of bimolecular and termolecular reactions are in cm³ s⁻¹ and cm⁶ s⁻¹, respectively; those of (4) and (9) are corrected for the higher third-body efficiency of CO₂ than Ar and N₂, respectively. $3.27 + 10 = 3.27 \times 10^{10} \text{ cm}^{-2} \text{ s}^{-1}$ scaled to the lower boundary of 47 km. CR (Cl) are column rates of the chlorine analogs from Krasnopolsky (2012).

However, our upper limit is applicable for the uniform distribution of HBr. Here we will try to obtain constraints on the HBr abundance in the lower atmosphere from our observation and the model. Venus albedo is 0.028 at 3.66 μm (Krasnopolsky 2010), much smaller than 0.85 at 600 nm and 0.7 at 2.25 μm because of the H₂SO₄ absorption. Single scattering approximation is reasonable for such a black atmosphere in our observation at 3.84 μm. Assuming the aerosol scale height of 3 and 4 km above 70 km and a constant extinction coefficient at 60–70 km, the calculated upper limits to HBr below 60 km are 70 and 20 ppb, respectively. The aerosol optical depth that fits to the observed CO₂ (Fig. 3) is 0.75 and 0.58 at 70 km, respectively, in accord with $\tau = 1$ at 69 ± 1 km at 2.5 μm (Cottini et al., 2015) and at 70.2 ± 0.8 km at 1.5 μm (Fedorova et al., 2016).

Thus, our observation results in the upper limits to HBr of 1 ppb at 78 km or 20–70 ppb below 60 km. Overall, the remote infrared spectroscopy is not favorable for detection of HBr because it does not sound the atmosphere below the cloud tops, where HBr is much more abundant (if it is) than above. In situ measurements at future descent probes and balloons may be better to solve this problem.

HBr has the greatest bond energy and is expected as a dominant bromine species in the lower atmosphere. Br₂ dissociates at $\lambda < 620$ nm, and this light penetrates into the atmosphere down to the surface (Ekonomov et al., 1983). Atomic bromine reacts with H₂S, which abundance is predicted at 150 ppb near the surface by the chemical kinetic model (Krasnopolsky 2013):

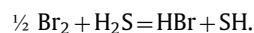


Rate coefficient of the direct reaction is $1.4 \times 10^{-13} e^{-2750/T} \approx 3 \times 10^{-13} \text{ cm}^3 \text{ s}^{-1}$ at 700 K (Nicovich et al., 1992). The constant of thermodynamic equilibrium is 0.8 at 700 K using thermodynamic parameters from Chase (1998), and

$$\frac{\text{HBr}}{\text{Br}} \approx 0.8 \frac{\text{H}_2\text{S}}{\text{SH}} \approx 2 \times 10^5$$

according to the model. This confirms our expectation based on the bond energies.

The upper limit of 0.2 ppb to Br₂ at 15 km (Moroz et al., 1981) may be also used to estimate abundance of HBr that is relevant to this limit using thermodynamic equilibrium



The calculated equilibrium constant is 7×10^{-5} at 735 K near the surface, and 0.2 ppb of Br₂ coupled with the model data for H₂S and SH results in an upper limit of 25 ppm to HBr in the lower atmosphere. Therefore our upper limit of 20–70 ppb to HBr in the lower atmosphere is significantly more restrictive for the bromine chemistry than the limit of 0.2 ppb to Br₂ at 15 km.

The derived upper limit to HBr may be compared with the observed abundances of HCl and HF. Nightside observations of the window at 1.75 μm by three teams (Bezard et al., 1990; Pollack et al. 1993; Iwagami et al. 2008) resulted in HCl ≈ 500 ppb at 15–30 km. Four observations of HCl near the cloud tops give HCl ≈ 400 ppb (Connes et al., 1967; Young 1972; Krasnopolsky 2010; Sandor and Clancy 2012) and one observation 750 ppb (Iwagami et al. 2008). Models for the lower atmosphere predict a constant HCl mixing ratio from the surface to the cloud layer. Photochemical models predict a weak decrease in the HCl mixing ratio from 400 ppb in the clouds to ≈320 ppb above 100 km because of a partial substitution of HCl by atomic chlorine. Submillimeter observations by Sandor and Clancy (2012) show a significant decrease from HCl ≈ 400 ppb at 70 km to 0–200 ppb at 90 km. SOIR/VEX occultations demonstrate an increase from 30 (20–100) ppb at 70 km to 300 (100–700) at 90 km and 800 (300–1700) ppb at 105 km (Mahieux et al. 2015). Here we give mean values for low latitudes and total ranges of the observed variations. The SOIR observations near 70 km disagree by an order of magnitude with those of eight teams at the cloud tops and in the lower atmosphere and require an unidentified source at 105 km and sink at 70 km.

Observations of HF were made by three teams at the cloud tops (Connes et al., 1967; Bjoraker et al., 1992; Krasnopolsky 2010) with a mean value of 5 ppb. Nightside observations in the window at 2.3 μm by two teams (Bezard et al., 1990; Pollack et al. 1993) gave 4 ppb at 30–40 km. The SOIR/VEX occultations show 5 (2.5–10) ppb at 80 km increasing to 50 (30–70) ppb at 103 km (Mahieux et al. 2015). Again, the SOIR/VEX data require a source at 103 km and a sink near 80 km. However, the mean value at 80 km agrees with the other observations.

While the chlorine chemistry initiated by HCl is basic for the Venus atmosphere, effects of HF and related chemistry are neglected in the photochemical models. There are a few reasons for this neglect. First of all, it is expected that chemistry of fluorine is rather similar to that of chlorine. Furthermore, HF is less abundant than HCl on Venus by two orders of magnitude. Finally, photolysis of HF is shifted to the far UV relative that of HCl and significantly blocked by the CO₂ absorption.

Relative abundances of F, Cl, and Br in the numbers of atoms are similar in the Sun and chondrites (Lodders 2003): Cl is more abundant than Br by a factor of 460. This factor is 560 in the bulk Earth composition (Wänke and Dreibus 1988). Scaling of the HCl mixing ratio of 400 ppb by the Br/Cl ratios in the Earth and the Sun, the expected HBr mixing ratios are 0.7 and 0.9 ppb, respectively, much smaller than the observed upper limit for the lower atmosphere (20–70 ppb).

The Cl/F ratio is evaluated at 6.2 in the Sun and chondrites (Lodders 2003) and 1.2 in the Earth (Wänke and Dreibus 1988). Surprisingly the solar ratio is rather close to that observed by

SOIR/VEX on Venus. Considering 400 ppb as a preferable mixing ratio of HCl and comparing it with that of HF, we come to the obvious conclusion that reactions of rocks that release and consume hydrogen halides (Fegley and Treiman 1992) determine their atmospheric mixing ratios, and the bulk abundances of elements are not the only factors that affect these species in the atmosphere.

6. Conclusions

To search for HBr on Venus, the strongest line of the strongest band HBr (1–0) R2 2605.8/6.2 cm^{-1} was observed using the NASA IRTF and a high-resolution long-slit spectrograph CSHELL with resolving power of 4×10^4 . 101 spectra of Venus have been analyzed and revealed HBr abundances varying from -8 to $+5$ ppb. Their mean is -1.2 ppb, standard deviation is 2.5 ppb, and uncertainty of the mean is 0.25 ppb. The negative value presumes a systematic error, and an estimated upper limit to HBr mixing ratio at the cloud tops of Venus is ~ 1 ppb. Using the retrieved CO_2 abundances, this limit refers to 78 km for a uniform distribution of HBr.

A simplified version of the bromine photochemistry is included into the photochemical model. Photolysis of HBr and its reactions with O and H deplete the HBr mixing ratio at 70–80 km relative to that below 60 km by a factor of ≈ 300 . Reanalysis of the observational data with the calculated profile of HBr gives an upper limit of 20–70 ppb for HBr below 60 km and aerosol optical depth of ≈ 0.7 at 70 km and $3.84 \mu\text{m}$.

The bromine chemistry may be effective on Venus even under the observed upper limit. However, if a Cl/Br ratio in the Venus atmosphere is similar to that in the Solar System, then HBr is ≈ 1 ppb in the lower atmosphere and the bromine chemistry is insignificant. Thermodynamic calculations based on the chemical kinetic model predict HBr as a major bromine species in the lower atmosphere.

Acknowledgments

This work is supported by Grant 16-12-10559 of the Russian Science Foundation to Moscow Institute of Physics and Technology (PhysTech).

References

- Atkinson, R., et al., 2007. Evaluated kinetic and photochemical data for atmospheric chemistry: Volume III – gas phase reactions of inorganic halogens. *Atmos. Chem. Phys.* 7, 981–1191.
- Baulch, D.L., Duxbury, J., Grant, S.J., Montague, D.C., 1981. Evaluated kinetic data for high temperature reactions. Volume 4 homogeneous gas phase reactions of halogen- and cyanide- containing species. *J. Phys. Chem. Ref. Data* 10.
- Bezard, B., de Bergh, C., Crisp, D., Maillard, J.P., 1990. The deep atmosphere of Venus revealed by high-resolution nightside spectra. *Nature* 345, 508–511.
- Bjoraker, G.L., Larson, H.P., Mumma, M.J., Timmermann, R., Montani, J.L., 1992. Airborne observations of the gas composition of Venus above the cloud tops: Measurements of H_2O , HDO, HF and the D/H and $^{18}\text{O}/^{16}\text{O}$ isotope ratios. *Bull. Amer. Astron. Soc.* 24, 995.
- Chase Jr., M.W., 1998. NIST-JANAF Thermodynamic Tables 9, 1–1951.
- Connes, P., Connes, J., Benedict, W.S., Kaplan, L.D., 1967. Traces of HCl and HF in the atmosphere of Venus. *Astrophys. J.* 147, 1230–1237.
- Cottini, V., Ignatiev, N.J., Piccioni, G., Drossart, P., 2015. Water vapor near Venus cloud tops from VIRTIS-H/Venus express observations 2006–2011. *Planet. Space Sci.* 113–114, 219–225.
- DeMore, W.B., et al., 1997. Chemical Kinetics and Photochemical Data for use in Stratospheric Modeling. JPL Publication, pp. 97–104. Evaluation Number 12.
- Donohoue, D.L., Bauer, D., Cossairt, B., Hynes, A.J., 2006. Temperature and pressure dependent rate coefficients for the reaction of Hg with Br and the reaction of Br with Br: a pulsed laser photolysis-pulsed laser induced fluorescence study. *J. Phys. Chem. A* 110, 6623–6632.
- Ekonomov, A.P., Golovin, Yu.M., Moroz, V.I., Moshkin, B.E., 1983. Solar scattered radiation measurements by Venus probes. In: Hunten, D.M., Colin, L., Donahue, T.M., Moroz, V.I. (Eds.), *Venus*. Univ. Arizona Press, pp. 632–649.
- Farmer, C.B., Norton, R.H., 1989. In: *Atlas of the Infrared Spectrum of the Sun and the Earth Atmosphere from Space*, vol. I. The Sun. NASA Ref. Publication, p. 1224.
- Fedorova, A., Marcq, E., Luginin, M., Korablev, O., Bertaux, J.L., Montmessin, F., 2016. Variations of water vapor and cloud top altitude in the Venus' mesosphere from SPICAV/VEX observations. *Icarus* 275, 143–162.
- Fegley, B., Treiman, A.H., 1992. Chemistry of atmosphere–surface interactions on Venus and Mars. In: Luhmann, J., Pepin, R.O. (Eds.), *Venus and Mars: Atmospheres, Ionospheres, and Solar Wind Interactions*, 66. Geophysical Monograph, pp. 7–71.
- Greene, T.P., Tokunaga, A.T., Toomey, D.W., Carr, J.S., 1993. A high spectral resolution 1–5 μ Cryogenic Echelle Spectrograph for the IRTF. *Proc. SPIE Int. Soc. Opt. Eng.* 1946, 313–320.
- Iwagami, N., et al., 2008. Hemispheric distributions of HCl above and below the Venus' clouds by ground-based 1.7 μm spectroscopy. *Planet. Space Sci.* 56, 1424–1434.
- Krasnopolsky, V.A., 2010. Spatially-resolved high-resolution spectroscopy of Venus. 1. Variations of CO_2 , CO, HF, and HCl at the cloud tops. *Icarus* 208, 539–547.
- Krasnopolsky, V.A., 2012. A photochemical model for the Venus atmosphere at 47–112 km. *Icarus* 218, 230–246.
- Krasnopolsky, V.A., 2013. S_3 and S_4 abundances and improved chemical kinetic model for the lower atmosphere of Venus. *Icarus* 225, 570–580.
- Krasnopolsky, V.A., 2017a. On the iron chloride aerosol in the clouds of Venus. *Icarus* 286, 134–137.
- Krasnopolsky, V.A., 2017b. Disulfur dioxide and its near-UV absorption in the photochemical model of Venus atmosphere. *Icarus*.
- Kurucz, R.L., 2011. <http://kurucz.harvard.edu/sun/atmos/>.
- Lodders, K., 2003. Solar system abundances and condensation temperatures of the elements. *Astrophys. J.* 591, 1220–1247.
- Mahieux, A., et al., 2015. Hydrogen halides measurements in the Venus mesosphere retrieved from SOIR on board Venus express. *Planet. Space Sci.* 113–114, 264–274.
- Mitchell, T.J., Gonzalez, A.C., Benson, S.W., 1995. Very low pressure reactor study of the $\text{H} + \text{HBr} = \text{H}_2 + \text{Br}$ reaction. *J. Phys. Chem.* 99, 16960–16966.
- Moroz, V.I., Golovin, Yu.M., Moshkin, B.E., Ekonomov, A.P., 1981. Spectrophotometric experiment on the Venera 11 and 12 descent probes. 3. Results of the spectrophotometric measurements. *Cosmic Res.* 19, 599–612.
- Nicovich, J.M., Kreutter, K.D., Van Dijk, C.A., Wine, P.H., 1992. Temperature-dependent kinetics studies of the reactions $\text{Br}(^2\text{P}_{3/2}) + \text{H}_2\text{S} = \text{SH} + \text{HBr}$ and $\text{Br}(^2\text{P}_{3/2}) + \text{CH}_3\text{SH} = \text{CH}_3\text{S} + \text{HBr}$. Heats of formation of SH and CH_3S radicals. *J. Phys. Chem.* 96, 2518–2528.
- Pollack, J.B., et al., 1993. Near-infrared light from Venus' nightside: a spectroscopic analysis. *Icarus* 103, 1–42.
- Rothman, L.S., et al., 2013. The HITRAN 2012 molecular spectroscopic database. *J. Quant. Spec. Rad. Tran.* 130, 4–50.
- Sander, S.P., et al., 2011. Chemical Kinetics and Photochemical Data for use in Atmospheric Studies. JPL Publication, pp. 10–16. Evaluation Number 17.
- Sandor, B., Clancy, R.T., 2012. Observations of HCl altitude dependence and temporal variation in the 70–100 km mesosphere of Venus. *Icarus* 220, 618–626.
- Seiff, A., et al., 1985. Models of the structure of the atmosphere of Venus from the surface to 100 km altitude. *Adv. Space Res.* 5, 3–58.
- Wänke, H., Dreibus, G., 1988. Chemical composition and accretion history of terrestrial planets. *Phil. Trans. R. Soc. Lond. A* 325, 545–557.
- Young, L.D.G., 1972. High resolution spectra of Venus: a review. *Icarus* 17, 632–658.